Colloids and Surfaces A: Physicochem. Eng. Aspects 338 (2009) 93–101

Contents lists available at ScienceDirect

Colloids and Surfaces A: Physicochemical and Engineering Aspects

journal homepage: www.elsevier.com/locate/colsurfa

Self-assembly characteristics of gold nanoparticles in the presence of cysteine

Aurora Mocanu[a], Ileana Cernica[b], Gheorghe Tomoaia[c], Liviu-Dorel Bobos[a], Ossi Horovitz[a,*], Maria Tomoaia-Cotisel[a]

[a] Babes-Bolyai University of Cluj-Napoca, Faculty of Chemistry and Chemical Engineering, Physical Chemistry Department, Arany J. Str., no. 11, 400028 Cluj-Napoca, Romania
[b] National Institute of Research and Development for Microtechnology of Bucharest, Erou Iancu Nicolae Str., no. 126 A, 077190 Voluntari, Romania
[c] Iuliu Hatieganu University of Medicine and Pharmacy, Orthopaedics and Traumatology Department, Traian Mosoiu Str., no. 47, 400015 Cluj-Napoca, Romania

ARTICLE INFO

Article history:
Received 21 September 2008
Received in revised form
23 November 2008
Accepted 30 December 2008
Available online 9 January 2009

Keywords:
Gold nanoparticles
Cysteine
UV–vis spectroscopy
TEM
AFM
DLS
Zeta potential

ABSTRACT

Gold nanoparticles in aqueous dispersions were prepared by two methods, using sodium citrate as reduction agent, and their interaction with L-cysteine was investigated. UV–vis, dynamic light scattering (DLS) and zeta potential measurements were used for physical and chemical characterization of mixtures with different gold:cysteine ratios, coupled with transmission electron microscopy (TEM) and atomic force microscopy (AFM) observations. Even a diluted (0.001 M) cysteine solution leads to a rapid assembly of gold nanoparticles and a broad absorption band at longer wavelength (characteristic for the aggregation of gold nanoparticles) develops and surpasses rapidly the peak of non-aggregated gold particles. TEM images for gold nanoparticles mixed with a 0.001 M cysteine solution show randomly arranged aggregates of gold nanoparticles on TEM carbon coated copper grids. AFM images indicate a rather ordered surface of self-assembled monolayers deposited on silanized glass. From thermodynamic considerations on the protolytic equilibria in aqueous cysteine solutions, the species present at different pH values were ascertained. A possible model for cysteine binding to gold nanoparticles and for the formation of gold particle assemblies is also suggested.

1. Introduction

As a consequence of the new discoveries by interdisciplinary research teams working with gold nanoparticles, related to potential applications in the field of nanotechnology, self-assembly, catalysis and molecular electronics, the interest for these systems is continuously increasing. Particularly, biofunctionalized and self-assembled gold nanoparticles are in the focus of research in biomedical and bioanalytical areas, such as controlled drug delivery, medical diagnosis and biosensors [1–6].

Amino acids are considered as suitable agents in the biofunctionalization of gold nanoparticles, as protective layers and for their assembly, due to the presence of different functional groups, such as –SH and $–NH_2$, with affinity for gold. Therefore, an amino acid, containing both functional groups, such as L-cysteine, is a promising compound to be used in this study for biofunctionalization of gold nanoparticles and for the mediation of their assembly with gold surfaces. Even more, amino acid capped gold surfaces are considered to represent the simplest mimics for protein surfaces [7].

Generally, amino acids can be adsorbed on the gold particle surface already during the formation of particles, using the amino acid itself as reduction agent [8–10], or in a latter stage, by ligand exchange reactions or binding on the former adsorbed stabilizing molecules [11–15]. Amino acids can also be used in the assembly formation of gold nanoparticles and for the design of biological surfaces for sensing and for nanoclusters based devices [16]. The properties of such assemblies could be designed rationally by choosing the initial amino acid [11].

The binding of cysteine to gold nanoparticles was communicated [12] and a review on amino acid interactions with metallic nanoparticles was given [13]. Among the amino acids, used as reduction and capping agents for silver or gold nanoparticles, are found cysteine, leucine and asparagine [10]. Further, the S–Au interaction in cysteine capped gold nanoparticels was discussed [10,14,15] and the binding of cysteine to Au was compared with that of leucine and asparagine [10]. Gold–silver nanocomposites were prepared from gold nanorod seeds in amino acid solutions, such as arginine, cysteine, glycine, glutamine, glutamate, histidine, lysine, or methionine [17]. Moreover, cysteine adsorbed on a gold surface was used to immobilize protein molecules [18–20].

In previous works, we synthesized gold nanoparticles in aqueous solutions of citrate and used them to be functionalized with various biomolecules, such as globular protein extracted from aleurone cells of barley [21] and amino acids, namely lysine [22].

The aim of the present investigation is to gain insights into the assembly formation of gold nanoparticles and interparticle inter-

* Corresponding author. Tel.: +40 264593833; fax: +40 264590818.
E-mail address: ossihor@yahoo.com (O. Horovitz).

0927-7757/$ – see front matter © 2009 Elsevier B.V. All rights reserved.
doi:10.1016/j.colsurfa.2008.12.041

actions in the presence of L-cysteine, which could have potential application for the analytical detection of amino acids found in various media. This investigation concerns the effect of cysteine concentrations on the surface plasmon resonance (SPR) band evolution of gold nanoparticles. On the other hand, the cysteine mediated aggregates of gold nanoparticles are visualized via TEM and AFM images and further characterized by DLS and zeta potential measurements.

2. Materials and methods

Two colloidal gold solutions were prepared by Au(III) reduction with sodium citrate.

Sample 1 was obtained by a variant of the Turkevich method [21,22], as adapted from Chah et al. [23]. The 200 ml 0.005% (w/w) $HAuCl_4{\cdot}3H_2O$ solution stirred vigorously was refluxed. To the boiling solution 15.3 mg trisodium citrate ($Na_3C_6H_5O_7{\cdot}2H_2O$), solved in a minimum amount of water, was added. After color change, the heat was turned off and the solution was allowed to cool overnight at room temperature. The gold content in the final dispersion is 25 mg/l.

Sample 2 was prepared by a method adapted from [24,25]. An 0.0175% aqueous solution of gold chloride (80 ml) and a mixture of 4 ml 1% $Na_3C_6H_5O_7{\cdot}2H_2O$, 1 ml 1% tannic acid, 1 ml 25 mM potassium carbonate and 14 ml H_2O were separately warmed up to 60 °C and then mixed while stirring. After the red color appeared (almost instantly) the mixture was heated up to 95 °C under stirring and then cooled on ice. The gold content in the final dispersion is 91 mg/l. Both resulting solutions of colloidal gold particles were stored in brown bottles and kept at 4 °C.

The tetrachloroauric (III) acid and $AuCl_3$ were purchased from Merck (high purity, above 99.5%). The trisodium citrate dihydrate ($Na_3C_6H_5O_7{\cdot}2H_2O$) was obtained from Sigma–Aldrich (high purity, above 99%). Tannic acid, pure powder, was purchased from Merck. K_2CO_3 pro analysis was obtained from Reactivul Bucharest. L-Cysteine was purchased from Merck (high purity). The 3-aminopropyl-triethoxysilane was purchased from Sigma and is of minimum 98% purity. All chemicals were used without further purification.

L-Cysteine was dissolved in deionized water in order to prepare 0.001, 0.01 and 0.1 M solutions. Deionized water with resistivity of 18 MΩ cm was used in all experiments and it was obtained from an Elgastat water purification system.

The UV–vis absorption spectrum of the solutions was studied using a Jasco UV/Vis V-530 spectrophotometer, with 10 mm path length quartz cuvettes in the 190–900 nm wavelengths range.

The investigated mixtures were obtained from the gold colloidal solution (having the given concentration c_{Au}) and the amino acid solutions (concentration c_{Cys}), by successive removal of small amounts of the previous mixture and adding of equal amounts of amino acid solution. The gold and amino acid content ratios reported to (c_{Au}/c_{Cys}) are given in the figures representing their spectra.

The gold nanoparticles dispersions (viz. sample 1 or sample 2) and their mixtures with cysteine solutions were adsorbed for 2 min on the specimen grids and air dried. In the presence of cysteine, the adsorption on grid was started 5 min after the mixing. The samples were observed with a transmission electron microscope (TEM: JEOL—JEM 1010). The TEM grids consist of carbon coated copper grids freshly prepared prior to use. TEM images have been recorded with a JEOL standard software.

Atomic force microscopy (AFM) investigations were executed on nanostructured films made by self-assembly from colloidal solutions containing gold nanoparticles both in the absence and the presence of cysteine, using a commercial AFM JEOL 4210 equipment, operating in tapping mode [26] at ambient conditions. The self-assembled nanostructured gold films were prepared by adsorption of gold nanoparticles on glass plates, 2 cm × 2 cm, that were optically polished and silanized with 3-aminopropyl-trietoxysilane prior to use [27].

For gold nanoparticles functionalized with cysteine, first, the colloidal gold solutions (viz. sample 1 or sample 2) were mixed with a cysteine solution. After the mixing, at a chosen time (e.g., 5 min), the silanized glass plates were immersed into the colloidal mixture and kept for 2 min or 60 min. The adsorbed amount of gold nanoparticles was monitored through the variation of the adsorption duration. The glass plates were placed in the colloidal mixture with the active silanized surface orientated vertically or horizontally facing down in order to prevent gold nanoparticles deposition through sedimentation. After the selected adsorption time, the plates were taken out from the colloidal mixture and rinsed thoroughly with deionized water to remove the excess adsorbed molecules.

For each sample, there were made two identical preparations, because two different washing modes were applied. A washing procedure was used by adding 5 ml of deionized water, directly to the bulk solution when the plate was still kept in contact with that solution, stirring gently, pumping 5 ml of solution, adding again 5 ml of water, and repeating these last steps five times, in order to eliminate the other solution ingredients adsorbed on the sample.

For the other series of preparations, after the adsorption time, the samples were gently taken out from bulk colloidal solutions and another washing procedure was applied by adding water (about 25 ml) on slightly tilted substrates, with adsorbed layers on them.

Afterwards, all rinsed samples were dried slowly in air, being dust protected, and used for AFM examination. No significant differences were observed for the two different washing procedures indicating that the adsorbed gold nanoparticles layers have good adhesion and are rather stable on silanized glass surface.

Standard cantilevers, non-contact conical shaped tips of silicon nitride coated with aluminum, were used. The sharpened tips were on cantilevers with a resonant frequency in the range of 200–300 kHz and with a spring constant of 17.5 N/m.

AFM observations were repeated on different areas from 10 μm × 10 μm to 1 μm × 1 μm of the same film. The images were obtained from at least 10 macroscopically separated areas on each sample. All images were processed using the standard procedures for AFM. AFM images consist of multiple scans displaced laterally from each other in y-direction with 512 × 512 pixels. All AFM experiments were carried out under ambient laboratory conditions (about 20 °C) as previously reported [28,29].

The Malvern Zetasizer Nano-ZS was used in order to estimate the particle size (e.g., hydrodynamic diameter) by dynamic light scattering (DLS [30,31]) and for the zeta potential measurements by laser Doppler electrophoresis. The measurements were executed on the colloidal gold solution (sample 2) and on mixtures in the 1:1 volume ratio of this sample with 10^{-3} M and respectively 10^{-2} M L-cysteine solutions. For the two mixtures, the measurements were made at 5 min after the mixing of the solutions, at 25 °C. For each sample, three measurements were executed at 2 min intervals.

3. Theory and calculations

3.1. Thermodynamics of protolytic equilibria for cysteine

Cysteine (three-letter code: Cys, one-letter code: C) is an amino acid with a thiol group (–SH) on the side chain (Fig. 1). It is a neutral, polar amino acid, with only limited hydrophilic properties [32]. Its pK_a values are 1.96 (for the carboxylic group), 8.18 (for the amine group) and 10.28 (for the thiol group) [33]. The isoelectric pH is 5.07 (the average of the first two pK values, which correspond to equilibria involving the neutral zwitterion).

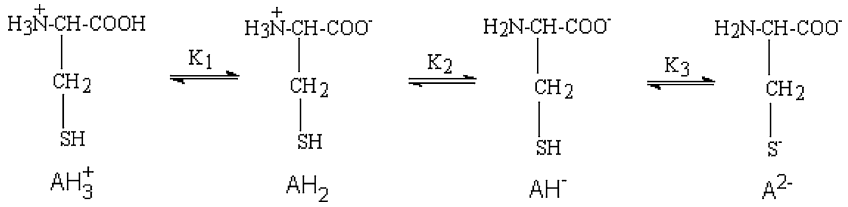

Fig. 1. Cysteine protolytic equilibria and corresponding thermodynamic constants taken from [33]. pK_1 = 1.96 (carboxylic group), pK_2 = 8.18 (α-amine group) and pK_3 = 10.28 (for thiol terminal group). Symbols are given for cysteine species in aqueous solutions.

The protonation equilibria of cysteine in aqueous solutions are given in Fig. 1.

Let us assume the total concentration of cysteine (species AH_3^+, AH_2, AH^- and A^{2-}) to be 1, and the concentrations of the different species to be $(1-x-y-z)$, x, y and z respectively; $[H^+] = h$. The equilibrium constants will be

$$K_1 = \frac{[AH_2][H^+]}{[AH_3^+]} = \frac{xh}{1-x-y-z} \quad (1)$$

$$K_2 = \frac{[AH^-][H^+]}{[AH_2]} = \frac{yh}{x} \quad (2)$$

$$K_3 = \frac{[A^{2-}][H^+]}{[AH^-]} = \frac{zh}{y} \quad (3)$$

We find successively:

From Eq. (3): $z = K_3 y/h$.
From Eq. (2): $y = K_2 x/h$ so $z = K_2 K_3 x/h^2$.
From Eq. (1): $xh = K_1 - K_1 x - K_1 K_2 x/h - K_1 K_2 K_3 x/h^2$.

$$z = \frac{K_1K_2K_3}{K_1K_2K_3 + K_1K_2h + K_1h^2 + h^3} = \frac{1}{1 + (h/K_3) + (h^2/K_2K_3) + (h^3/K_1K_2K_3)} \quad (4)$$

$$y = \frac{K_1K_2}{K_1K_2 + K_1h + K_1K_2K_3/h + h^2} = \frac{1}{1 + (h/K_2) + (h^2/K_1K_2) + (K_3/h)} \quad (5)$$

$$x = \frac{K_1}{K_1 + K_1K_2/h + K_1K_2K_3/h^2 + h} \quad (6)$$

or, in terms of pK and pH:

$$[A^{2-}] = z = \frac{1}{1 + 10^{-pH+pK_3} + 10^{-2pH+pK_2+pK_3} + 10^{-3pH+pK_1+pK_2+pK_3}} \quad (7)$$

$$[AH^-] = y = \frac{hz}{K_3} = z \times 10^{-pH+pK_3} \quad (8)$$

$$[AH_2] = x = \frac{hy}{K_2} = y \times 10^{-pH+pK_2} \quad (9)$$

$$[AH_3^+] = 1 - x - y - z \quad (10)$$

The curves giving the concentrations (mole fractions) of the different protonated species of cysteine versus pH are shown in Fig. 2. The neutral zwitterionic form of cysteine is stable in the pH range from 3 to 7, the cationic form only at a pH under 0. The double negative anionic form (having the thiol group deprotonated) is stable above pH 12, while the mononegative anionic form has a very narrow stability domain, at pH about 9. At our working pH (about 5) the neutral species of cysteine (AH_2) is therefore the only one present.

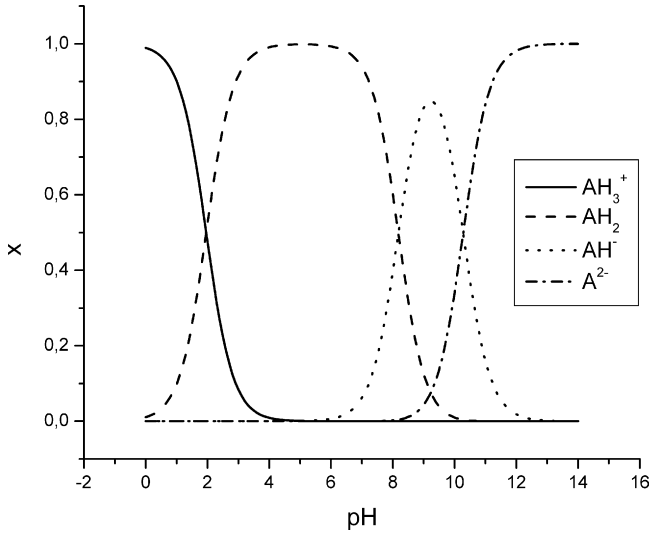

Fig. 2. Mole fractions (X) of cysteine species: $[AH_3^+]$, $[AH_2]$, $[AH^-]$ and $[A^{2-}]$, as a function of pH of aqueous solutions.

4. Results and discussion

4.1. Characterization of colloidal gold solutions

The visible absorption spectra of the gold aqueous colloidal solutions present a well-defined absorption band with a maximum at the wavelength λ_{max} = 527–528 nm (sample 1) [21] and respectively 521–522 nm (sample 2). These values are characteristic for plasmon absorbance for nanometric Au particles. The lower value for the absorption maximum of sample 2 suggests it should contain lower sized particles.

The size of the colloidal gold particles has been measured by TEM imaging. Two representative TEM images for the two samples of these gold particles are given in Fig. 3. The particles show mostly spherical or ellipsoidal shape. It is evident that in sample 2 particles are smaller and the particle density is higher. From the sizes of a great number of particles, measured on the TEM images, the following characteristics of the colloidal gold samples were calculated and given in Table 1.

The histograms providing the size distribution of gold nanoparticles, obtained from TEM pictures are given in Fig. 4. For comparison, the curve indicating the expected normal distribution was added.

Table 1
Characteristics of gold nanoparticles and colloidal gold dispersions for sample 1 and sample 2.

Characteristics	Sample 1	Sample 2
Average size (diameter, nm)	14.2	6.9
Standard deviation (nm)	2.6	1.3
Extreme values of the sizes (nm)	8.5–24	3.2–10.6
Average mass of a particle (considered spherical) (g)	2.9×10^{-17}	3.3×10^{-18}
Number of gold atoms in a particle	8.8×10^4	10^4
Number of particles per cm^3 of solution	8.6×10^{11}	2.8×10^{13}

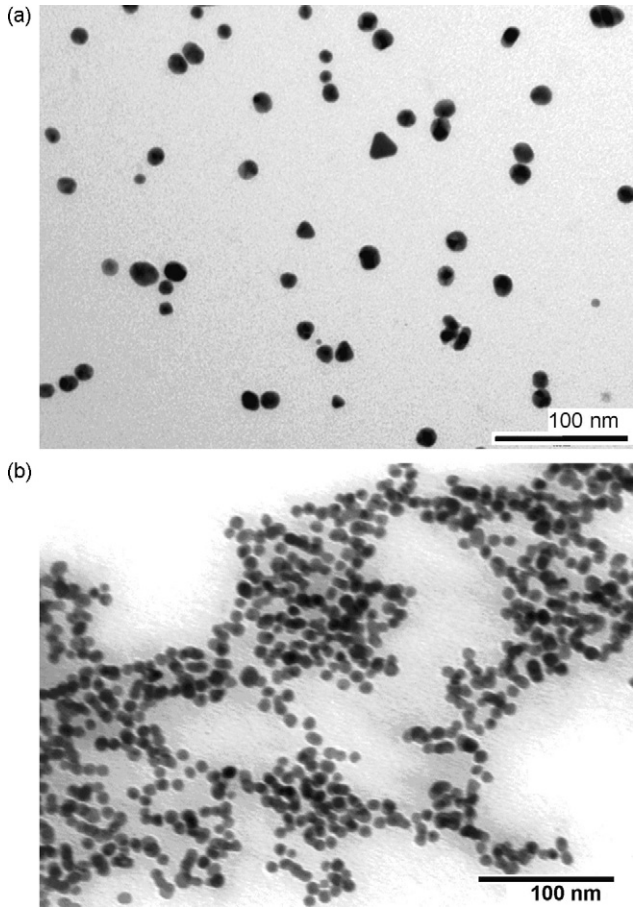

Fig. 3. TEM images of gold nanoparticles: sample 1 (a) and sample 2 (b).

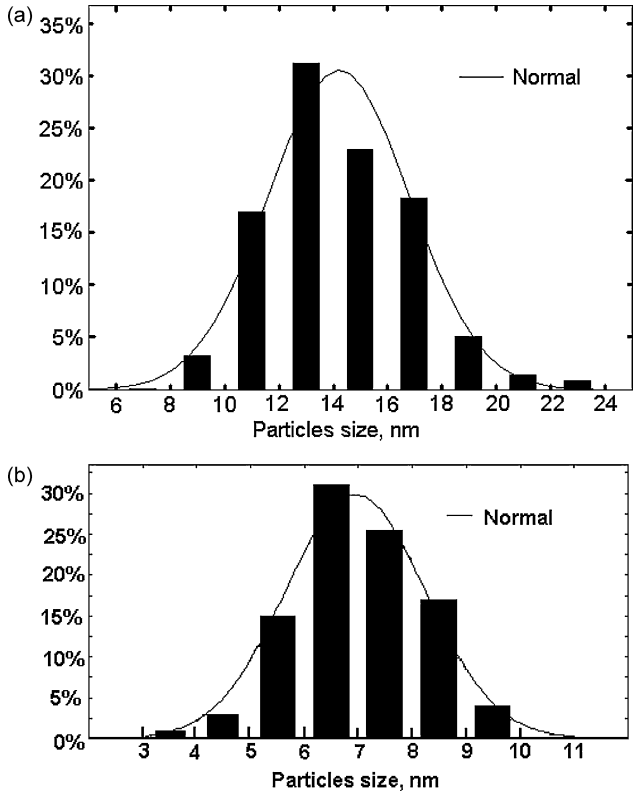

Fig. 4. Histograms of size distribution for gold particles: (a) sample 1 and (b) sample 2.

The deviations from the normal distribution are rather important for both samples, i.e. sample 1 (Fig. 4a) and sample 2 (Fig. 4b), which is plausible for such complex dispersions.

It is to be noted that in the preparation of sample 2, tannic acid was added just with the aim to obtain smaller gold nanoparticles. With increasing amounts of tannic acid, the mean size of the particles decreases. Tannic acid is itself a reducing agent and increases the rate of nucleation for gold nanoparticles, while potassium carbonate is added in order to neutralize the tannic acid.

Both colloidal gold solutions proved as very stable in time, without observable modifications in the UV–vis spectrum after preparation. This indicates electrostatic stabilization via nanoparticle surface-bound citrate anions and the gold nanoparticles are negatively charged.

Dynamic light scattering [30,31] was also used to characterize the colloidal gold solution (sample 2). The reported hydrodynamic diameter of the gold particles has an average value under 10 nm, with maxima at 7–8 nm for the size distribution, in substantial agreement with data given in the histogram of Fig. 4b. The average value for the zeta potential was $\zeta = -40.3$ mV.

4.2. Interactions of gold nanoparticles with cysteine

L-Cysteine has a strong effect on *UV–vis spectra* of gold nanoparticle solutions, more than other amino acids, for instance lysine

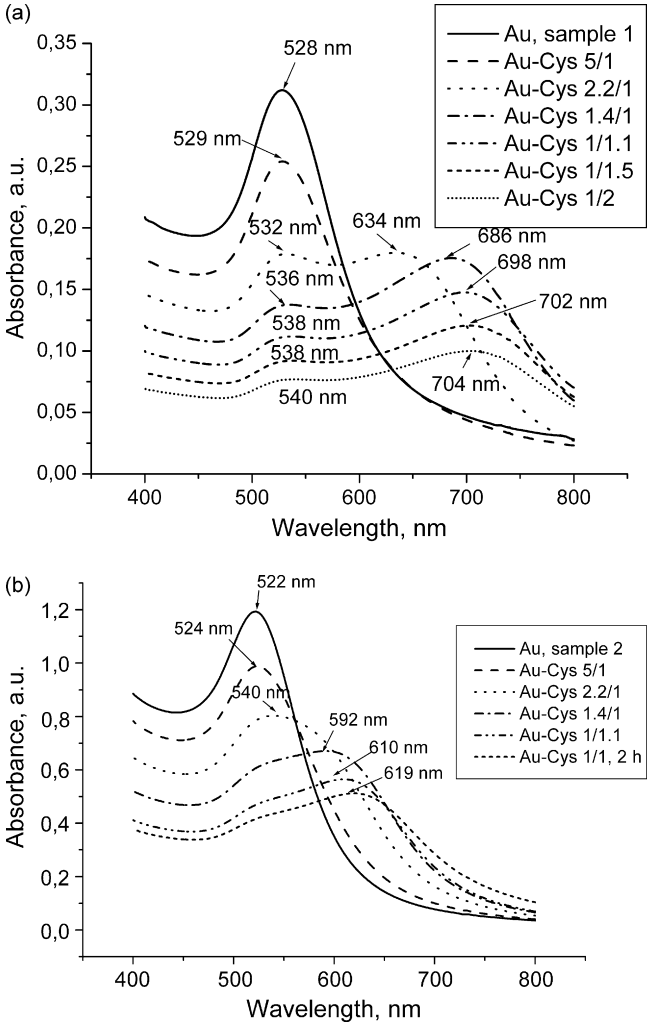

Fig. 5. Optical spectrum of gold solutions: sample 1 (a) and sample 2 (b) with 0.001 M cysteine solution in different ratios, expressed in terms of the c_{Au}/c_{Cys} ratio.

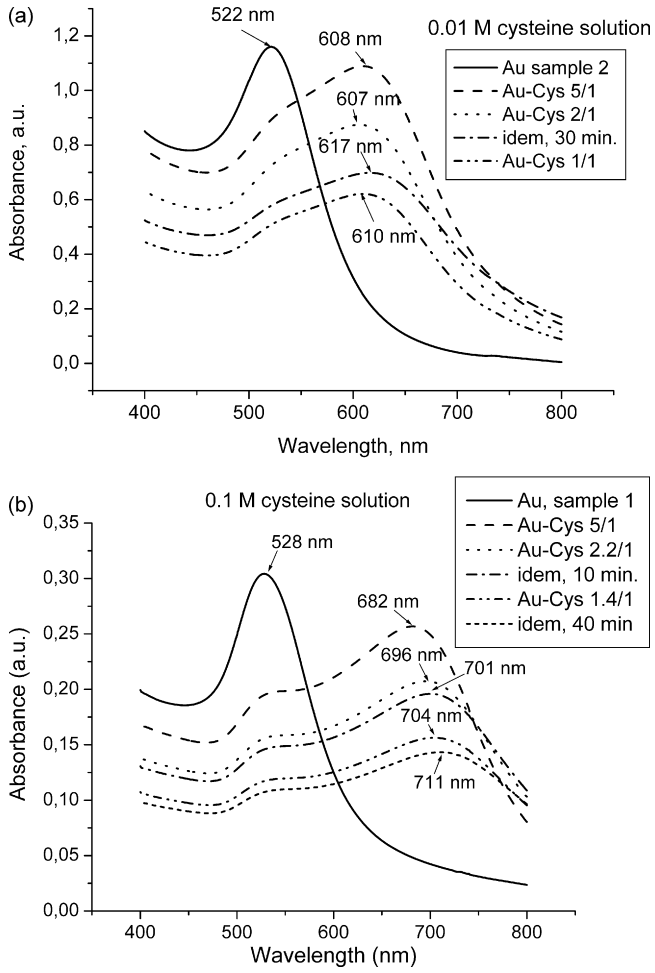

Fig. 6. Optical spectrum of gold solutions sample 2 with 0.01 M cysteine solution (a) and sample 1 with 0.1 M cysteine solution (b) in different ratios, expressed in terms of the c_{Au}/c_{Cys} ratio.

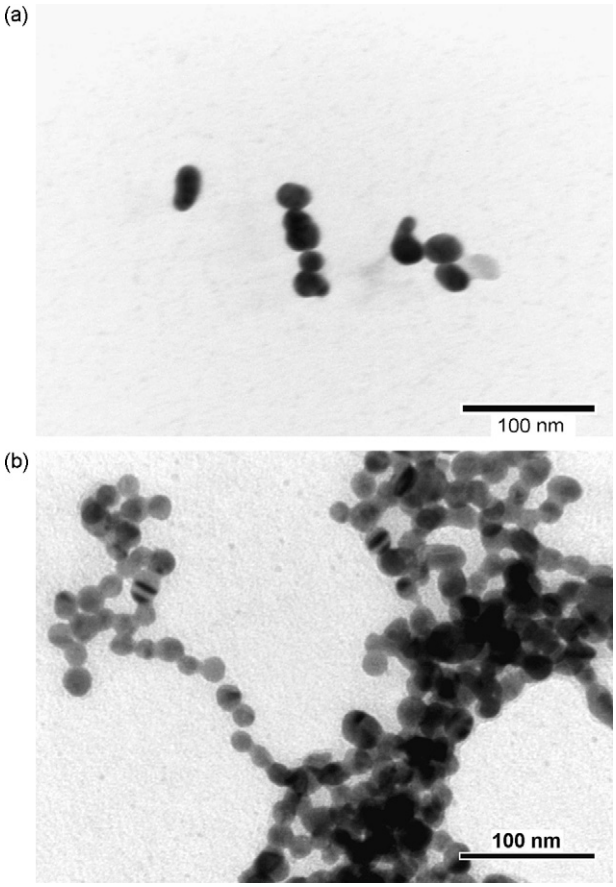

Fig. 7. TEM images of gold nanoparticles with 0.001 M cysteine solution: (a) sample 1 and (b) sample 2.

[22]. Already, a 10^{-3}-M solution (Fig. 5) added to the colloidal gold solutions leads to a rapid broadening of the adsorption peak, which is shifted towards higher wavelengths. It is known that the development of the broad peak at longer wavelengths in the UV–vis spectrum comes from the coupling of surface plasmon resonance of two adjacent nanoparticles and is an indication of the anisotropic optical properties of the gold nanoparticles aggregates [34]. The peak for the broad band at longer wavelength surpasses rapidly the peak of the initial non-aggregated gold particles and the maximum wavelength goes above 700 nm for sample 1 (Fig. 5a). The color of the solution changed from reddish to blue. For sample 2 (Fig. 5b), comprising smaller gold nanoparticles, the shift is less pronounced (till 620 nm). Finally, in the case of both samples after titration with cysteine, for the initial individual gold particles there is no peak, but only a shoulder. The additions of 0.01 M to sample 2 (Fig. 6a) and 0.1 M to sample 1 (Fig. 6b) cysteine solutions lead to the color change in blue already at the first amount added. From Figs. 5 and 6, a time evolution of aggregation is also visible.

This kind of color change as an effect of aggregation is a well-understood phenomenon [34–36]. When the interparticle distance in the aggregates decreases to less than about the average particle diameter, the electric dipole–dipole interaction and coupling between the plasmons of neighboring particles in the aggregates results in the bathochromic shift of the absorption band.

These results support the observations about the interaction of cysteine with gold nanoparticles [14], where, based on the analysis of FT-IR and Raman spectra, the authors affirm the existence of covalent interaction of sulphur and gold. The formation of a covalent bond Au–S is also assumed by other authors [15,37]. Further, it was suggested [38] that the positively charged amino group in cysteine ($-NH_3^+$) should interact with the negative charge on the surface of other gold nanoparticles through electrostatic binding, thus forming assemblies.

Furthermore, the band broadening and the shift of the surface plasmon band were reported to reflect the advanced aggregation of gold nanoparticles with decreasing in pH values and by increasing the electrolyte concentration [14].

Also, our findings are in substantial agreement with reported data on the adsorption of homocysteine on gold nanoparticles [39], which data were applied in a detection method used to determine the homocysteine concentrations in biological liquids [40].

TEM images for gold nanoparticles functionalized with 0.001 M cysteine solution (volume ratio 1:1) show agglomerated gold nanoparticles (clusters), with random orientations, for sample 1 (Fig. 7a) and especially for sample 2 (Fig. 7b). For the higher particles concentration of sample 2, the clusters are also united in a more complex network (Fig. 7b). By comparing Fig. 7 with Fig. 3, it is observed that the cysteine had an effect of enlarging the size of gold nanoparticles of both samples. The effect is apparently stronger for sample 2 (Figs. 3b and 7b).

The *AFM images* for gold nanoparticles functionalized with cysteine, adsorbed on silanized glass, evidence the self-assembly of gold nanoparticles in Fig. 8 (sample 1) and Fig. 9 (sample 2). A tendency towards clusters (aggregates) is also evident from these AFM

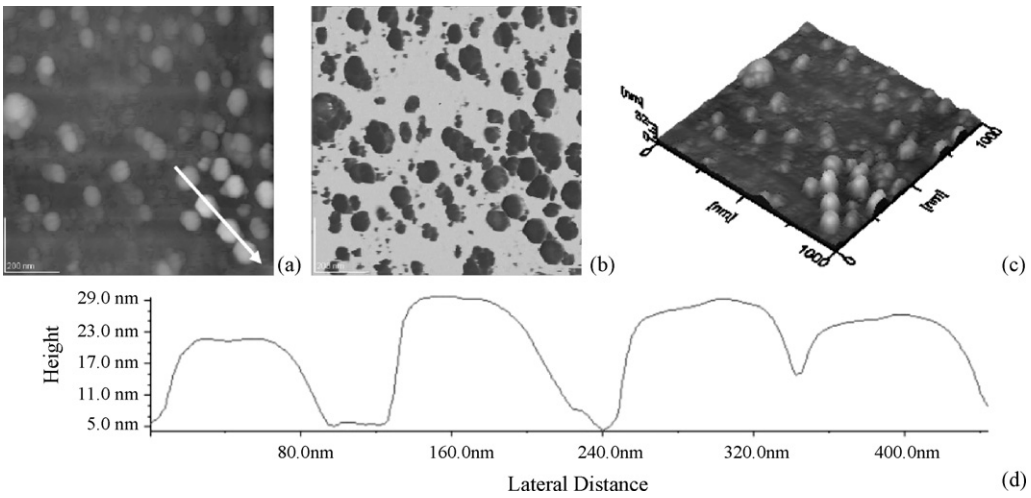

Fig. 8. (a) 2D-topographic and (b) phase AFM images of the assembly of gold nanoparticles (sample 1), mediated by 0.01 M cysteine, on silanized glass after 1 h adsorption time; scanned area 1000 nm × 1000 nm; 3D-view (c) of the topography (a); (d) cross-section profile along the arrow in panel (a).

images as compared with the gold nanoparticles (sample 2) without cysteine, adsorbed on the same solid support (Fig. 10), and in substantial agreement with TEM observations (Fig. 7).

The self-assembly aggregates visualized by TEM (Fig. 7) and AFM (Figs. 8 and 9) confirm the results found by UV–vis investigation (Figs. 5 and 6).

Briefly, both AFM topography and phase images show the structure of gold nanoparticles assemblies obtained within 2 min (Fig. 9) for sample 2 in the presence of 0.001 M cysteine, and in 60 min (Fig. 8) for sample 1 with 0.01 M cysteine.

The AFM images evidenced a variety of structures, including linear arrangement, distorted pentagons and hexagons and randomly packed nanoparticles. Generally, the arrangements could be generated by the interactions among particles and clusters, and between them and the silanized glass surface, during the course of adsorption from colloidal solution and assembly on solid surface. Nevertheless, the complex structure of self-assembled gold nanoparticles is probably influenced by drying patterns. To diminish the drying artifacts, the AFM samples were slowly dried and dust protected.

Further, the analysis of cross-sections, given in Figs. 8d and 9d, evidences the aggregates of gold nanoparticles. When gold nanoparticles are to close to each other, the tip convolution effects with the film surface might lead apparently to slightly bigger gold nanoparticles (Figs. 8 and 9). However, it is clear that the increases in both the adsorption time and in cysteine concentration had an effect of enlarging the size of gold nanoparticles aggregates. Thus, it can be established that AFM is suitable for monitoring the aggregation process during the self-assembly formation.

Therefore, TEM and AFM investigations showed a possible transfer of gold nanoparticles functionalized with L-cysteine from colloidal solutions to solid substrates.

The *DLS measurements* for the mixtures of colloidal gold solution (sample 2) with cysteine solutions evidenced a relatively high degree of polydispersion; the distribution maximum appears at 15–20 nm for the 10^{-3} M cysteine solutions and at 25 nm for the 10^{-2} M cysteine solution (at 5 min after mixing), but it is shifted (in this latter case) to about 40 nm (10 min after mixing). This result indicates a time evolution of the particles self-aggregation. These measurements support the TEM and AFM observations in substantial agreement with spectroscopic data.

The *zeta potential measurements* give a mean value of −40.3 mV for the gold colloidal solution (sample 2), while for the mixtures of gold nanoparticles and cysteine solutions the zeta potential is less

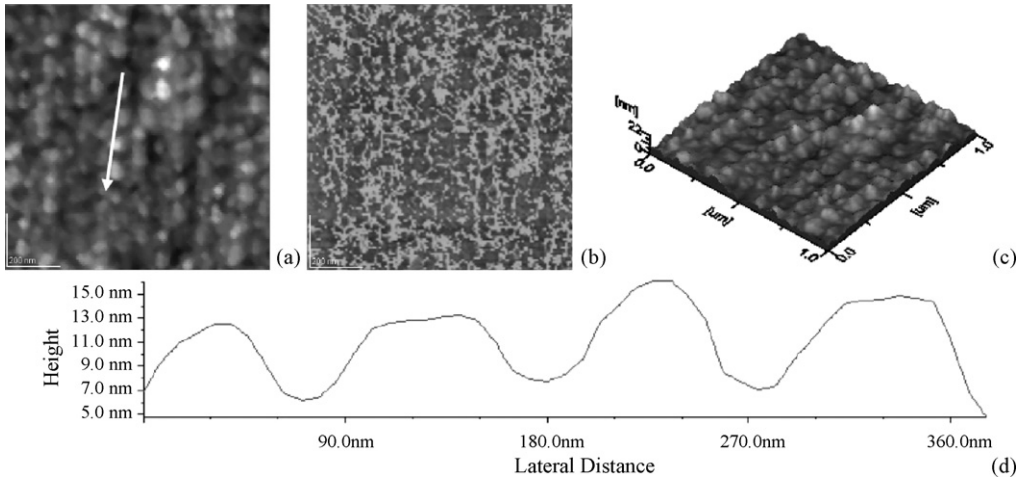

Fig. 9. (a) 2D-topographic and (b) phase AFM images of the assembly of gold nanoparticles (sample 2), mediated by 0.001 M cysteine, on silanized glass after 2 min adsorption time; scanned area 1000 nm × 1000 nm; 3D-view (c) of the topography (a); (d) cross-section profile along the arrow in panel (a).

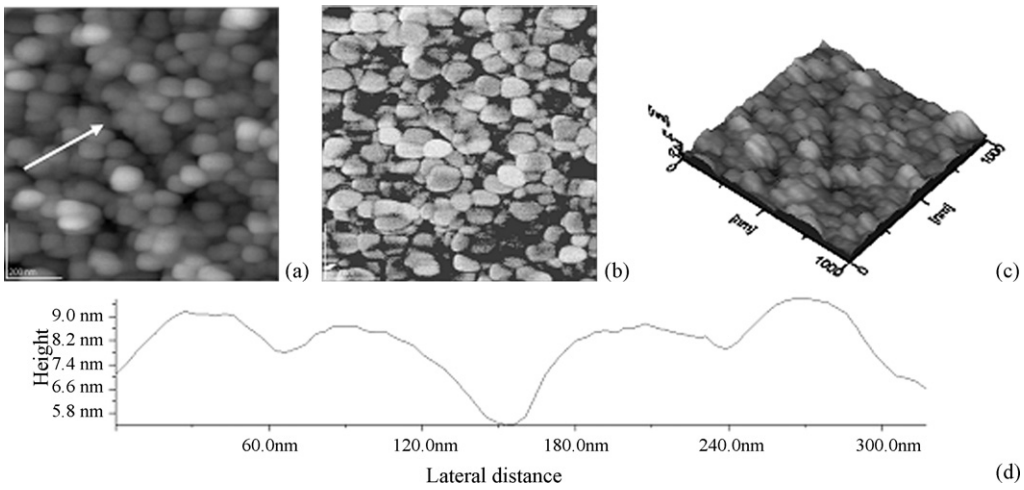

Fig. 10. (a) 2D-topographic and (b) phase AFM images of gold nanoparticles (sample 2), on silanized glass after 1 h adsorption time; scanned area 1000 nm × 1000 nm; 3D-view (c) of the topography (a); (d) cross-section profile along the arrow in panel (a).

negative. In the case of the mixture with 10^{-3} M cysteine solution in 1:1 volume ratio it becomes −32.5 mV, and for the more concentrated (10^{-2} M) cysteine solution it amounts to only −25.3 mV. For the latter solution it passes under the 30 mV value, which is usually considered as the limit assuring the stability of colloidal systems [41]. Therefore, the addition of cysteine reduces the (negative) surface charge of the gold nanoparticles, thus, increasing their tendency for aggregation.

4.3. Model of cysteine binding to gold nanoparticles

Cysteine is probably bound to the gold nanoparticles by its thiol (–SH) group, as was also suggested by the study of ^{1}H NMR spectra [10,14]. This bond is formed by ligand exchange reactions between cysteine and citrate capped gold nanoparticles. A possible model illustrating both the cysteine bindings to gold nanoparticles and the formation of particle aggregates is schematized in Fig. 11. After cys-

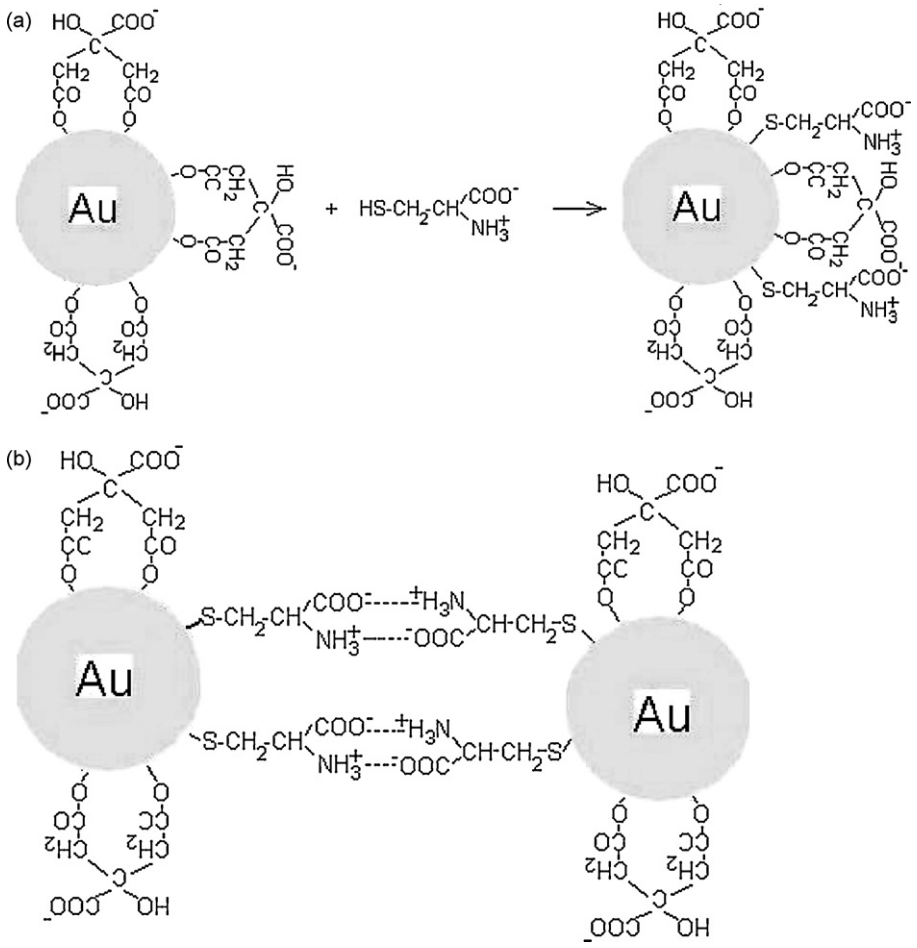

Fig. 11. Schema of cysteine binding to citrate capped gold nanoparticles (a) and of bonds formation between gold nanoparticles (b).

teine adsorption on the gold nanoparticles, the cysteine molecule has still two functional groups free to form bonds between particles.

We note that the interaction between cysteine and citrate bound to gold nanoparticles cannot be ruled out [36,42]. The positive amine group of cysteine is capable to form salt bridges with carboxylate from citrate adsorbed on gold nanoparticles.

Besides the electrostatic interaction mechanism by salt bridges, a possible formation of hydrogen bonds between surface bonded cysteine molecules of neighboring cysteine capped gold nanoparticles is also mentioned [43].

5. Conclusions

UV–vis spectroscopy, DLS, zeta potential, TEM and AFM are applied to investigate the self-assembly characteristics of gold nanoparticles with cysteine.

Our data indicate that the assembly of gold nanoparticles can be induced by cysteine, an amino acid possessing an additional thiol functional group besides the alpha-amine. The cysteine assembly effect could be explained primarily through the zwitterion-type electrostatic interactions between the charged amine and acid groups of cysteine molecules, bound to the gold nanoparticles by their –SH groups. The affinity of S-atoms for gold makes cysteine more effective than other amino acids in adsorption process on gold nanoparticles.

This affinity of gold nanoparticles towards cysteine, as well as towards other amino acids, can lead to the development of new detection methods for analytical purposes, medical diagnostics and biosensors and to potential controlled drug delivery applications. On the other hand, the use of cysteine both in the functionalization of gold nanoparticles and in the cross-linking of amino acid capped gold nanoparticles leading to stable self-assemblies are promising ways to the synthesis of nanostructured biomaterials with important implications in nanoscience and nanotechnology.

Acknowledgement

This research was carried out with financial support from the Romanian Ministry of Education and Research (Scientific research project no. 5, within the Excellency Research Program).

References

[1] M. Zheng, X. Huang, Biofunctionalization of gold nanoparticles, in: C.S.S.R. Kumar (Ed.), Biofunctionalization of Nanomaterials, Wiley–VCH, Chichester, 2005, pp. 99–124.
[2] D. Fitzmaurice, S. Connolly, Programmed assembly of gold nanocrystals in aqueous solutions, Adv. Mater. 11 (1999) 1202–1205.
[3] S. Mann, W. Shenton, M. Li, S. Connolly, D. Fitzmaurice, Biologically programmed nanoparticle assembly, Adv. Mater. 12 (2000) 147–150.
[4] M.C. Daniel, D. Astruc, Gold nanoparticles: assembly, supramolecular chemistry, quantum-size-related properties, and applications toward biology, catalysis, and nanotechnology, Chem. Rev. 104 (2004) 293–346.
[5] N.L. Rosi, C.A. Mirkin, Nanostructures in biodiagnostics, Chem. Rev. 105 (2005) 1547–1562.
[6] J.C. Love, L.A. Estroff, J.K. Knebel, R.G. Nuzzo, G.M. Whitesides, Self-assembled monolayers of thiolates on metals as a form of nanotechnology, Chem. Rev. 105 (2005) 1103–1170.
[7] C.C. You, M. De, G. Han, V.M. Rotello, Tunable inhibition and denaturation.of α-chymotrypsin with amino acid-functionalized gold nanoparticles, J. Am. Chem. Soc. 127 (2005) 12873–12881.
[8] P. Selvakannan, S. Mandal, S. Phadtare, A. Gole, R. Pasricha, S.D. Adyanthaya, M. Sastry, Water-dispersible tryptophan-protected gold nanoparticles prepared by the spontaneous reduction of aqueous chloraurate ions by the amino acid, J. Colloid Interf. Sci. 269 (2004) 97–102.
[9] S.K. Bhargava, J.M. Booth, S. Agrawal, P. Coloe, G. Kar, Gold nanoparticle formation during bromoaurate reduction by amino acids, Langmuir 32 (2005) 5949–5956.
[10] S. Aryal, B.K. Remant, B. Narayan, C.H. Kim, H.Y. Kim, Study of electrolyte induced aggregation of gold nanoparticles capped by amino acids, J. Colloid Interf. Sci. 299 (2006) 191–197.
[11] L. Xu, Y. Guo, R. Xie, J. Zhuang, W. Yang, Three-dimensional assembly of Au nanoparticles using dipeptides, Nanotechnology 13 (2002) 725–728.
[12] J. Zsang, Q. Chi, J.U. Nielsen, E.P. Friis, J.E.T. Andersen, J. Ulstrup, Two-dimensional cysteine and cystine cluster networks on Au(1 1 1) disclosed by voltammetry and in situ scanning tunneling microscopy, Langmuir 16 (2000) 7229–7237.
[13] S. Mandal, S. Phadtare, M. Sastry, Interfacing biology with nanoparticles, Curr. Appl. Phys. 4 (2005) 118–127.
[14] S. Aryal, B.K.C. Remant, N. Dharmaraj, N. Bhattarai, C.H. Kim, H.Y. Kim, Spectroscopic identification of S–Au interaction in cysteine capped gold nanoparticles, Spectrochim. Acta A 63 (2006) 160–163.
[15] Z.P. Li, X.R. Duan, C.H. Liu, B.A. Du, Selective determination of cysteine by resonance light scattering technique based on self-assembly of gold nanoparticles, Anal. Biochem. 351 (2006) 18–25.
[16] A.K.A. Aliganga, I. Lieberwirth, G. Glasser, A.-S. Duwez, Y. Sun, S. Mittler, Fabrication of equally oriented pancake shaped gold nanoparticles by SAM-templated OMCVD and their optical response, Org. Electron. 8 (2007) 161–174.
[17] Y.F. Huang, Y.W. Lin, H.T. Chang, Growth of various Au–Ag nanocomposites from gold seeds in amino acid solutions, Nanotechnology 17 (2006) 4885–4894.
[18] P. Tengvall, M. Lestelius, B. Liedberg, I. Lundstroem, Plasma protein and antisera interactions with L-cysteine and 3-mercaptopropionic acid monolayers on gold surfaces, Langmuir 8 (1992) 1236–1238.
[19] Y.C. Sasaki, K. Yasuda, Y. Susuki, T. Ishibashi, I. Satoh, Y. Fujiki, S. Ishiwata, Two-dimensional arrangement of a functional protein by cysteine–gold interaction: enzyme activity and characterization of a protein monolayer on a gold substrate, Biophys. J. 72 (1997) 1842–1848.
[20] I. Willner, E. Katz, B. Willner, R. Blonder, V. Heleg-Shabtai, A.F. Bückmann, Assembly of functionalized monolayers of redox proteins on electrode surfaces: novel bioelectronic and optobioelectronic systems, Biosens. Bioelectron. 12 (1997) 337–356.
[21] O. Horovitz, A. Mocanu, Gh. Tomoaia, L. Olenic, Gh. Mihăilescu, O. Boroştean, A. Popoviciu, C. Crăciun, T. Yupsanis, M. Tomoaia-Cotisel, Synthesis, characterization and properties of gold nanoparticles in colloidal aqueous solutions in the absence and in the presence of globular proteins. Auto-assembled gold nanostructures in thin films, in: M. Zaharescu, E. Burzo, L. Dumitru, I. Kleps, D. Dascalu (Eds.), Convergence of Micro–Nano-Biotechnologies, Romanian Academy Press, Bucharest, 2006, pp. 132–146.
[22] O. Horovitz, A. Mocanu, Gh. Tomoaia, L. Bobos, D. Dubert, I. Dăian, T. Yupsanis, M. Tomoaia-Cotisel, Lysine mediated assembly of gold nanoparticles, Studia Univ. Babes-Bolyai Chem. 52 (2007) 97–108.
[23] S. Chah, M.R. Hammond, R.N. Zare, Gold nanoparticles as a colorimetric sensor for protein conformational changes, Chem. Biol. 12 (2005) 323–328.
[24] J.W. Slot, H.J. Geuze, Sizing of protein A—colloidal gold probes for immunoelectron microscopy, J. Cell Biol. 90 (1981) 533–536.
[25] J.W. Slot, H.J. Geuze, A new method of preparing gold probes for multiple-labeling cytochemistry, Eur. J. Cell Biol. 38 (1985) 87–93.
[26] K.S. Birdi, Scanning Probe Microscopes. Applications in Science and Technology, CRC Press, New York, 2003.
[27] O. Seitz, M.M. Chehimi, E. Cabet-Deliry, S. Truong, N. Felidj, C. Perruchot, S.J. Greaves, J.F. Watts, Preparation and characterisation of gold nanoparticle assemblies on silanised glass plates, Colloids Surf. A: Physicochem. Eng. Aspects 218 (2003) 225–239.
[28] M. Tomoaia-Cotisel, The nanostructure formation of the globular seed storage protein on different solid surfaces studied by atomic force microscopy, in: M. Zaharescu, E. Burzo, L. Dumitru, I. Kleps, D. Dascalu (Eds.), Convergence of Micro–Nano-Biotechnologies, Romanian Academy Press, Bucharest, 2006, pp. 147–161.
[29] O. Horovitz, Gh. Tomoaia, A. Mocanu, T. Yupsanis, M. Tomoaia-Cotisel, Protein binding to gold auto-assembled films, Gold Bull. 40 (4) (2007) 295–304.
[30] H. Xie, K.L. Gill-Sharp, D.P. O'Neal, Quantitative estimation of gold nanoshell concentrations in whole blood using dynamic light scattering, Nanomed.: Nanotechnol. Biol. Med. 3 (2007) 89–94.
[31] Y. Yeh, H.Z. Cummins, Localized fluid flow measurements with a He–Ne laser spectrometer, Appl. Phys. Lett. 4 (10) (1964) 176–178.
[32] M.J. Betts, R.B. Russell, Amino acid properties and consequences of substitutions, in: M.R. Barnes, I.C. Gray (Eds.), Bioinformatics for Geneticists, Wiley, Chichester, 2003.
[33] D.R. Lide, Handbook of Chemistry and Physics, 12th ed., CRC Press, Boca Raton, 1991.
[34] N.R. Jana, L. Gearheart, S.O. Obare, C.J. Murphy, Anisotropic chemical reactivity of gold spheroids and nanorods, Langmuir 18 (2002) 922–927.
[35] K.S. Mayya, V. Patil, M. Sastry, On the stability of carboxylic acid derivatized gold colloidal particles: the role of colloidal solution pH studied by optical absorption spectroscopy, Langmuir 13 (1997) 3944–3947.
[36] O. Horovitz, Gh. Tomoaia, A. Mocanu, T. Yupsanis, M. Tomoaia-Cotisel, Protein binding to gold colloids, Gold Bull. 40 (3) (2007) 213–218.
[37] P.K. Sudeep, S.T.S. Joseph, K.G. Thomas, Selective detection of cysteine and glutathione using gold nanorods, J. Am. Chem. Soc. 127 (2002) 6516–6517.
[38] U. Kreibig, L. Genzel, Optical absorption of small metallic particles, Surf. Sci. 156 (1985) 678–700.
[39] I.S. Lim, W. Ip, E. Crew, P.N. Njoki, D. Mou, C.J. Zhong, Y. Pan, S. Zhou, Homocysteine mediated reactivity and assembly of gold nanoparticles, Langmuir 23 (2007) 826–833.
[40] C. Ku, Y. Zu, V. Wing-WahYam, Specific post-column detection method for HLPC assay of homocysteine based on aggregation of fluorosurfactant-capped gold nanoparticles, Anal. Chem. 79 (2007) 666–672.

[41] R.J. Hunter, Zeta Potential in Colloid Science: Principles and Applications, Academic Press, UK, 1988.
[42] S.H. Brewer, W.R. Glomm, M.C. Johnson, M.K. Knag, S. Franzen, Probing BSA binding to citrate-coated gold nanoparticles and surfaces, Langmuir 21 (2005) 9303–9307.
[43] V. Patil, R.B. Malvankar, M. Sastry, Role of particle size in individual and competitive diffusion of carboxylic acid derivatized colloidal gold particles in thermally evaporated fatty amine films, Langmuir 15 (1999) 8197–8206.